STING/NF-κB/IL-6-mediated inflammation in microglia contributes to spared nerve injury (SNI)-induced neuropathic pain

Jia Sun
Tongji Hospital of Tongji Medical College of Huazhong University of Science and Technology
Ya-Qun Zhou
Tongji Hospital of Tongji Medical College of Huazhong University of Science and Technology
Bing-Yang Xu
Tongji Hospital of Tongji Medical College of Huazhong University of Science and Technology
Jia-Yan Li
Tongji Hospital of Tongji Medical College of Huazhong University of Science and Technology
Long-Qing Zhang
Tongji Hospital of Tongji Medical College of Huazhong University of Science and Technology
Jia-Yi Wu
Tongji Hospital of Tongji Medical College of Huazhong University of Science and Technology
Shao-Jie Gao
Tongji Hospital of Tongji Medical College of Huazhong University of Science and Technology
Dai-Qiang Liu
Tongji Hospital of Tongji Medical College of Huazhong University of Science and Technology
Pei-Xiang Lan
Tongji Hospital of Tongji Medical College of Huazhong University of Science and Technology
Da-Wei Ye
Tongji Hospital of Tongji Medical College of Huazhong University of Science and Technology
Wei Mei (wmei@hust.edu.cn)
Tongji Hospital https://orcid.org/0000-0001-6556-6628

Research

Keywords: double-stranded DNA, interferon gene stimulator, microglia, neuropathic pain

Posted Date: February 9th, 2021

DOI: https://doi.org/10.21203/rs.3.rs-201560/v1

Abstract

Background

Innate immune response acts as a first line of host defense against damage and are initiated following the recognition of pathogen-associated molecular patterns (PAMPs). For double-stranded DNA (dsDNA) sensing, interferon gene stimulator (STING) was discovered to be an integral sensor, and could mediate the immune and inflammatory response. However, it is unclear the underlying mechanisms of STING in the development of neuropathic pain.

Methods

Neuropathic pain model was established by spared nerve injury (SNI). STING agonist DMXAA was introduced into BV-2 cells to assess the inflammatory response in microglia cells. Selective STING antagonist C-176 were administered in the early and late stage following SNI and the mechanical sensitivity and thermal responsiveness were assessed using Von Frey filaments and hot plate tests separately. To investigate the underlying mechanisms, recombinant IL-6 was injected intrathecally and its downstream effectors were examined. The level of dsDNA in the peripheral blood following SNI was assessed using Elisa analysis. STING signaling pathway and its downstream effectors were assessed by qPCR, western blots, Elisa and immunofluorescence staining. Meanwhile, microglia activation and proinflammatory cytokines expression were also assessed in the spinal cord.

Results

We found dsDNA was significantly increased and STING signaling pathway was activated in dorsal horn microglia following SNI, and our study using BV-2 cells showed that DMXAA significantly activated STING/TANK-binding kinase 1 (TBK1)/nuclear factor-kappa B (NF-κB) pathway, and increased the production of proinflammatory cytokines, as well as phosphorylated the Janus-activated kinase 2/signal transducer activator of transcription 3 (JAK2/STAT3) signal in microglia. Early but not late intrathecal injection of C-176 attenuated SNI-induced pain hypersensitivity, microglia activation, proinflammatory factors and phosphorylated JAK2/STAT3 in the spinal cord dorsal horn. Last, the analgesic effect of C-176 were greatly abolished by recombinant IL-6 following SNI.

Conclusions

We provided evidence clarifying dsDNA mediated activation of microglial STING signaling pathway, after which promoting expression of proinflammatory cytokines that are required for central sensitization in the spinal cord dorsal horn of SNI model. Further analysis showed that microglial STING/TBK1/NF-κB

may contribute to hyperalgesia initiation via IL-6/JAK2/STAT3 signaling. Pharmacological blockade of STING may be a promising target during the initiation of neuropathic pain.

Introduction

Neuropathic pain is an complex disease process due to injury or disease affecting the somatosensory nervous system [1], markedly impairing the quality of life in patients globally. Innate immune response acts as first lines of host defense against damage or disease and are initiated following the recognition of pathogen-associated molecular patterns (PAMPs) [2, 3]. There is growing evidence indicated that pattern recognition receptors (such as Toll-like receptors), sense microbial nucleic acids and translating this into a central immune signal [3–5]. For double-stranded DNA (dsDNA) sensing, stimulator of interferon genes (STING) was discovered to be activated by endogenous and exogenous DNA and triggered the immune and inflammatory response [6]. STING, acts as a central immune molecule, usually in a state of self-inhibition and was found to predominantly located in the endoplasmic reticulum (ER) [7]. After activating, STING moved from ER to the Golgi apparatus and eventually reached the cytoplasmic punctate structures for assembly with TANK-binding kinase 1 (TBK1) [8]. Accumulating evidence elucidated that STING is a pro-inflammatory molecule in the cyclic GMP-AMP synthase (cGAS) -STING signaling pathway, and implicated in several neuroinflammatory conditions [9–12].

Neuroinflammation is a well-controlled physiological process that serves to promote tissue regeneration and wound healing, however, excessive or prolonged neuroinflammation may result in chronic pain. Immune cells and chemokines have been identified as potential biomarkers or pathophysiological factors in neuropathic pain states [13]. It is increasingly clear that a large number of cytokines and chemokines induced by peripheral and central immune cells could regulate pain receptors and modulate pain hypersensitivity [14–16]. Moreover, crosstalk between neuronal and non-neuronal immune cells in the central nervous system plays a pivotal role in initiating and maintaining the chronic pain stage [15–18]. Microglia are the primary non-neuronal immunocompetent cells in the spinal cord. Generally, microglia remain at rest (M0). Under stress, microglia can rapidly change morphology. The activated microglia can be polarized into proinflammatory M1 microglia (such as inducible nitric oxide synthase (iNOS), CD86, CD68, interleukin 1β (IL-1β), interleukin 6 (IL-6), monocyte chemotactic protein 1 (MCP-1) and tumor necrosis factor-α (TNF-α)), and immunosuppressive M2 microglia (such as arginase-1 and interleukin 10 (IL-10)) [19–22]. Studies have suggested the regulating of microglia towards M2 phenotype plays an important role in the spinal cord of neuropathic pain [23–26].

Given STING's critical role in immunoregulatory and inflammation, we hypothesized that STING was involved in neuroinflammation and subsequent induce pain hypersensitivity. Thus, in this study, we assessed the role of STING in the spinal cord using neuropathic pain models induced by SNI. We found that after sensing increased dsDNA, STING and its downstream signaling are activated in the spinal cord microglia following SNI, and microglial STING activation could promote microglia activation, and release pro-inflammatory cytokines, all of these consequent inducing pain hypersensitivity in the spinal cord.

Materials

Animals

Male C57BL/6J mice (6-8 weeks, 23-25 g) were used (Tongji Medical College, Wuhan, China). All mice were placed in a temperature-controlled environment, followed a 12-hour light-dark cycle, 50% humidity, and were randomly fed a standard diet and water. The experimental procedures were performed in accordance with the approval of the ethics committee of the Animal Care and Use Committee of Huazhong University of Science and Technology.

Drugs and anesthesia

All operations were conducted under 50 mg/kg sodium pentobarbital anesthesia (i.p.). STING inhibitor C-176 purchased from Selleck (Houston, TX, USA) was dissolved in corn oil for different concentration (2, 4, 8 μg/μl, respectively). Recombinant mice IL-6 from R&D Systems (Minneapolis, MN) was dissolved in Phosphate buffered saline (PBS). For rIL-6 injection, animals received a single injection of 100ng of mice rIL-6 at day 1 following SNI. The drugs were delivered intrathecally (i.t., 5 μl). The STING agonist DMXAA purchased from Selleck (Houston, TX, USA) was dissolved in Dimethyl sulfoxide (DMSO; AppliChem, Darmstadt, Germany), and 100 μg/ml of DMXAA was given in BV-2 cells.

SNI and behavioral tests

The model of SNI was established in this study. Under anesthesia, the left sciatic nerve of mice was exposed at the mid-thigh level, the three peripheral branches of the sciatic nerve (common peroneal, sural, and tibial nerves) were exposed without stretching muscles and nerves. A tight ligation (5-0 silk) and transection of tibial nerves and common peroneal nerves together, removing 2-3 mm length of the nerves distal to the ligation and leaving the sural nerve intact. The animals in the sham group underwent the same procedure without injury of the nerves. For acute or chronic treatment, mice were randomly divided into the following groups: (1) Sham group: sham-operated mice with vehicle injection (corn oil or PBS, 5 μl, i.t.); (2) SNI group: SNI-injured mice with vehicle injection (corn oil or PBS, 5 μl, i.t.); (3) SNI+ C-176 group: SNI-injured mice with C-176 injection (10, 20, 40 μg, i.t.); and (4) SNI+ C-176+ rIL-6 group: SNI-injured mice with C-176 (40 μg, i.t.) combined with rIL-6 (100 ng, i.t.) injection.

Mechanical allodynia was assessed by measurement of paw withdrawal threshold (PWT) using Von Frey filaments (Stoelting, Wood Dale, IL, USA) as previously described [27, 28]. In brief, mice were placed in separate chambers (10×10×15 cm) for 30 minutes before the test. Then, the tip of filaments was placed on the plantar surface of the left hind paw for 5 s per force. Ascending order of forces (0.007, 0.02, 0.04, 0.16, 0.4, 0.6, 1.0, 1.4 and 2g) were used, starting with 0.007 g and ending with 2 g. The duration of each force was maintained for approximately 1s. Quick paw lifting or licking was considered to be positive responses. PWTs were decided as the lowest force required to elicit a positive response [3-5].

Thermal hyperalgesia was determined by measurement of thermal withdrawal latency (TWL) using Hargreaves plantar test (Ugo Basile, Italy). In brief, mice were placed in separate chambers (10×10×15

cm) on a glass plate for 30 minutes before the test. The radiant heat source was applied beneath the plantar surface of the left hind paw and the stimulus shut off when the hind paw moved. Each hind paw was repeated 3 times with a period of 5-6 minutes intervals. The mean TWL was determined from the mean of three measurements. The maximum period was set at 30 seconds to avoid tissue damage. The glass plate was cleaned between each interval.

The Open Field Maze (OFM) was applied to assess movement. Mice were adapted in the laboratory for 30 min before the test. Then the mice were individually placed in the center of open field, which consisted of a plastic base (50×50×50 cm) and divided into 25 grids and the centric 9 grids of equal area were defined as central area. The total distance and speed were recorded.

Cell culture

The murine BV-2 cell lines were cultured in Dulbecco's modified Eagles medium (DMEM, Gibco, NY, USA) supplemented with 10 % fetal bovine serum (FBS, Yeasen, Uruguay, SA) at 37 ℃ with 100 % humidity in 5 % CO2 for 2 days. Then the cells were put into a 6-well plate or 12-well plate for further experiments. After 24 h, cells were treated with DMXAA (100 μg/ml) with another 24 h [29]. The supernatants were gathered for enzyme linked immunosorbent assay (ELISA) analysis and cells were processed for western blotting and immunostaining.

Real-time PCR

Under deep anesthesia, spinal cords of mice (L4-L5) were quickly removed for analysis. Total RNA was isolated with RNAiso Plus (Takara, Kyoto, Japan), and MCP-1, IL-1β and TNF-α mRNA expression were normalized to the β-actin. cDNA was then synthesized using HiScript II Q RT SuperMix for qPCR (Vazyme, Nanjing, China):

MCP-1- 5-CCACTACCTTTTCCACAACCA-3 (sense),

5-GGCATCACAGTCCGAGTCAC-3 (antisense);

IL-1β- 5-TGCCACCTTTTGACAGTGATG-3(sense),

5 -TGTGCTGCTGCGAGATTTG-3 (antisense);

TNF-α- 5 -GTCTACTGAACTTCGGGGTGAT-3 (sense),

5 -TGCTACGACGTGGGCTACA-3 (antisense);

β-Actin- 5-CTGAGAGGGAAATCGTGCGT-3 (sense),

5-CCACAGGATTCCATACCCAAGA-3 (antisense).

Western blotting

Under deeply anesthetized, the L4 -L5 spinal cord were quickly removed and homogenized on ice using lysis buffer containing a cocktail of protease inhibitors and protein inhibitors. The homogenates or cell lysates were separated by 10% SDS-PAGE and transferred to 0.45 μm PVDF membranes (Millipore, Billerica, MA, USA). The PVDF membranes were blocked with 5% skim milk or BSA at RT (room temperature) for 2 h. Then the primary antibodies were used: anti-STING (A3262; ABclonal, Wuhan, China), anti- Phospho-TBK1 (AP1026; ABclonal, Wuhan, China), anti-TBK1 (A2573; ABclonal, Wuhan, China), anti-Phospho-NF-κB (AP0123; Abcam, Cambridge, UK), anti-NF-κB (A19653; ABclonal, Wuhan, China), anti-iNOS (A0312; ABclonal, Wuhan, China), anti-CD68 (A13286; ABclonal, Wuhan, China), anti-CD86 (A19026; ABclonal, Wuhan, China), anti-Phospho-JAK2 (#3776; Cell Signaling Tech, MA, USA), anti-JAK2 (A11497; ABclonal, Wuhan, China), anti- Phospho-STAT3 (#9145; Cell Signaling Tech, MA, USA), anti-STAT3 (A11216; ABclonal, Wuhan, China), and anti-β-actin (AC026; ABclonal, Wuhan, China). The membranes were incubated with HRP-conjugated goat anti- rabbit IgG (H+L) (A21020, Abbkine, Wuhan, China) at RT for 2 h. The protein expression was detected using chemiluminescence (Bio-Rad, Hercules, CA) and quantified using System with a Molecular Imager (Bio-Rad, Hercules, CA).

ELISA

Under deep anesthesia, blood samples were collected from the inferior vena cava of mice and centrifuged for serum collection, dsDNA ELISA kit (ELK8414, ELK Biotechnology CO., LTD, Wuhan, China) were used for measuring the levels of dsDNA concentration in sera according to the manufacturer's instruction. Further, the L4-L5 spinal cord of mice were quickly removed and homogenized on ice-cold 0.01 mol/L PBS. The concentrations of interleukin-6 (IL-6) were measured in BV-2 cells culture supernatants and in the L4-L5 spinal cord of mice using IL-6 ELISA kit (RK00008, Abclonal, Wuhan, China). The concentrations of IFN-β were measured in the L4-L5 spinal cord of mice using IFN-β ELISA kit (ELK8414, ELK Biotechnology CO., LTD, Wuhan, China).

Immunofluorescence staining

Immunofluorescence staining was conducted as previously described [28]. Under deep anesthesia, mice having been intracardially perfused with 50 ml cold-PBS followed by 50 ml 4% cold-paraformaldehyde (PFA). The L4-5 segment of the spinal cord were collected and post-fixed in 4 % PFA overnight at 4 ℃. 20 μm sections of spinal cord were cut on a cryostat (CM1900, Leica, Heidelberg, Germany). The sections were penetrated with 0.3% TritonX-100 for 10 min and blocked with 5% donkey serum for 45 min at RT. Then the following primary antibodies were used: anti-STING (A3262; ABclonal, Wuhan, China.), anti-Phospho-TBK1 (AP1026; ABclonal, Wuhan, China); anti-neuronal nuclei antibody (NeuN, ab104224, Abcam, Cambridge, UK); anti-glial fibrillary acidic protein antibody (GFAP; 3670; Cell Signaling Technology, Danvers, MA, USA) and anti- Iba1 antibody (ab5076; Abcam, Cambridge, UK). After washing 6 times with PBS, the sections were incubated with donkey anti-rabbit secondary antibody (711-547-003; Jackson ImmunoResearch, PA, USA), donkey anti-mouse secondary antibody (715-585-150; Jackson ImmunoResearch, PA, USA), and donkey anti-goat secondary antibody (705-585-003; Jackson

ImmunoResearch, PA, USA) for 2 h at RT. The sections were captured by using a fluorescence microscope (DP70, Olympus, Japan).

For immunocytochemistry, BV-2 cells were washed with cold-PBS for 3 times and then fixed with 4 % PFA at RT for 15min. The following primary antibodies were used after treatment with 0.3 % Triton X-100 followed by 5 % donkey serum: anti-STING (A3262; ABclonal, Wuhan, China); anti-Phospho-TBK1 (AP1026; ABclonal, Wuhan, China); anti-Phospho-NF-κB (AP0123; Abcam, Cambridge, UK); anti-neuronal nuclei antibody (ab104224; Abcam, Cambridge, UK); anti-glial fibrillary acidic protein antibody (3670; Cell Signaling Technology, Danvers, MA, USA) and anti-Iba1 antibody (ab5076; Abcam, Cambridge, UK). After washing 3 times with PBS, cells were then processed with the secondary antibody (Alexa Fluor 488-conjugated donkey anti-rabbit secondary antibody; 711-547-003; Jackson ImmunoResearch, PA, USA) for 2 h at RT. After washing 4 times with PBS, the cells were then counterstained with DAPI for 7 min. Fluorescent images were then captured by using a fluorescence microscope (DP70, Olympus, Japan).

Experimental designs and animal groups

The experimental designs and animal groups have been exhibited as Fig. 1.

Experiment 1: Time course of pain behaviors and STING signaling expression following SNI.

Fifty mice were randomly assigned into sham or SNI group. The pain behaviors were measured at days 1, 3, 7, 14 after SNI surgery, and then, the L4-5 spinal cord was removed for Elisa, western blot, and immunofluorescent analysis.

Experiment 2: The effects of DMXAA on microglia cells.

After SNI surgery, STING and p-TBK1 was mainly colocalized with Iba1(microglia cells). Thus, the cultured BV2 cell was stimulated with DMXAA. Cells were assigned into control and DMXAA group. 24 h later, cells were obtained for real-time PCR, Elisa, western blot, and immunofluorescent analysis.

Experiment 3: The effects of C-176 on pain hypersensitivity and microglia activation following SNI.

After SNI surgery, fifty mice were divided into SNI+Vehicle and SNI+C-176 group. For early injection, C-176 was injected once daily from day 1 to day 5, and the pain behaviors were assessed 0.5h before injection and from day 1 to day 5; for late injection, C-176 was injected once daily from day 7 to day 11, and the pain behaviors were assessed 0.5h before injection and from day 7 to day 11. We found that early but not late C-176 injection could inhibit pain development following SNI. Thus, the L4-5 spinal cord was removed for further analysis following SNI at day 7 with or without C-176 injection by real time PCR, Elisa, western blot, and immunofluorescent analysis. Correspondingly, the L4-5 spinal cord of sham operated group was collected at day 7.

Experiment 4: The analgesic effects of C-176 was abolished by mice rIL-6 following SNI.

After SNI surgery, forty rats were divided into SNI+Vehicle, SNI+C-176 and SNI+ C-176+rIL-6 group. C-176 was given from day 1 to day 5 following SNI, and mice rIL-6 was simultaneously injected with C-176 at day 1, 3 and 5 in SNI+ C-176+rIL-6 groups. Mechanical allodynia was assessed 0.5h before injection and at day 7.

Statistics

All data are presented as means ± SEM and analyzed by GraphPad Prism version 6.0. Student's t test (two-tailed) was used for differences between two groups, one-way ANOVA followed by Bonferroni post hoc test was used for differences between multiple groups. Behavior results (such as PWT and TWL) were analyzed by two-way ANOVA with repeated measures, followed by Bonferroni post hoc test. $p < 0.05$ was indicated statistically significant.

Results

Temporal up-regulated and activated STING signaling following SNI.

We first examined the level of dsDNA in peripheral blood in mice. Elisa analysis showed that the level of dsDNA was significantly upregulated in SNI mice compared with sham group (Fig. 2A). As STING is a critical sensor of dsDNA, we next assessed the activation of the STING signaling pathway in L4-5 spinal cord dorsal horn. Western blot analyses showed that the expression of STING and phosphorylated TBK1 (p-TBK1) were increased as early as 3- day following SNI, peaked at 7- day, and declined thereafter (Fig. 2B and C). Phosphorylated nuclear factor-kappa B (p-NF-κB, p-p65) increased at day 1 and maintained at a high level from day 3 to day 14, whereas the levels remained low in sham mice (Fig. 2D). In parallel with the increased protein levels, STING and p-TBK1 immunoreactivity was increased at 7-day after SNI (Fig. 2E). These results indicated that dsDNA was increased following SNI and triggered early activation of STING signaling pathway.

STING signaling pathway mainly activated in microglia.

To identify the cellular distribution of STING signaling pathway in the spinal cord dorsal horn in more detail, we detected the localization of STING and TBK1 both before and after SNI surgery. STING was found mostly colocalized to Iba1 microglia (Fig. 3), and p-TBK1 was also mainly colocalized to Iba1 microglia following SNI (Fig. 4). Moreover, microglia activation marker Iba1 was increased at 7 day following SNI compared with sham group. These data showed that STING signaling pathway was significantly activated in the nociceptive pathway in the spinal cord microglia.

In order to examine the intracellular behavior of STING, a membrane-permeable mouse-specific STING agonist DMXAA was used in microglia- like BV-2 cells. In agreement with the response produced by dsDNA in SNI, DMXAA could significantly active STING signaling pathway (including STING, p-TBK1 and p-p65) (Fig. 5). Immunofluorescence analyses revealed that DMXAA obviously promoted the perinuclear translocation of STING (Fig. 5B) and triggered the nuclear translocation of p-TBK1 and p-p65 (Fig. 5D and

F), which was consistent with our western blot analysis. Meanwhile, we measured the levels of pro-inflammatory cytokines. As displayed in Fig. 6, the production of pro-inflammatory cytokines (iNOS, MCP-1, IL-1β, TNF-α, and IL-6) were significantly increased in DMXAA stimulated group (DMXAA group) compared with the control group (Control group), which play a critical role in central sensitization and further led to microglia activation and pro-inflammatory cytokines production [14-16, 30, 31]. One of the most significantly increased protein was IL-6, which could further activate the Janus-activated kinase 2/signal transducer activator of transcription 3 (JAK2/STAT3) transduction pathway in microglia and contribute to neuropathic pain [32, 33]. In our study, DMXAA significantly phosphorylated and up-regulated the JAK2/STAT3 signaling pathway (Fig. 6F), which indicated that STING was involved in the activation of the JAK2/STAT3 pathway in microglia. These results illustrated that STING was an upstream signaling molecule for producing pro-inflammatory cytokines which could further promote microglia activation and increase the phosphorylation level of JAK2/STAT3 in microglia.

SNI-induced pro-inflammatory cytokines in the spinal cord microglia.

Growing evidence suggested that microglia activation and subsequent release of proinflammatory cytokines were involved in hyperalgesia of SNI [30]. To elucidate the mechanisms of microglial STING participating pain in vivo, time-course of PWT, TWL, and proinflammatory cytokines were assessed in SNI-injured pain model. Results showed that pain hypersensitivity after SNI gradually developed from day 1 to day 3, and was fully established after day 7 in ipsilateral hind paw (Fig. 7A and B). The pretreatment values were similar between sham and SNI group. Consistently, M1 markers including iNOS, CD68, CD86, IL-6 in the dorsal horn were significantly increased following SNI. INOS increased at day 3 and peaked at day 7 following SNI (Fig. 7C). CD68, CD86 and IL-6 increased at day 3 and were maintained at a high level from day 7 to day 14 following SNI, whereas the levels remained low in sham mice (Fig. 7D, E and F). These results showed that mechanical allodynia, thermal hyperalgesia was decreased, and proinflammatory cytokines was upregulation at early time points following SNI. Notably, IFN-β, a key component of type I IFN, was significantly increased at day 14 (Fig. 7G), which seems to play a dominant role in the maintaining of pathological pain states [34].

Early C-176 administration attenuated pain hypersensitivity

In order to explore the potential role of STING in pain development, the selective STING antagonist C-176 was used. For acute treatment, a single dose of C-176 (10, 20, 40 μg), or vehicle (corn oil, 5 μl) was given intrathecally (i.t.) at day 1. PWT and TWL were conducted at 0, 0.5, 1, 2, 4, 8h after C-176 injection. Data showed that C-176 could upregulate both PWT and TWL at 0.5 h, peaked at 1 h and lasted at least 8 h (Fig. 8A, Supplementary Figure S1A). For successive administration, C-176 (10, 20, 40 μg), or vehicle (corn oil, 5 μl) was given once daily from day1 to day 5, the behavioral tests were also performed at 1h after C-176 injection from day 1 to day 5. Repeated injection of C-176 significantly increased both PWT and TWL with no sign of tolerance in SNI mice (Fig. 8B, Supplementary Figure S1B).

Next, we assess the role of STING in the maintenance of neuropathic hypersensitivity. Single injection of C-176 at day 7 could also upregulate both PWT and TWL at 0.5 h, peaked at 1 h and lasted at least 8 h

(Fig. 8C, Supplementary Figure S1C). Then, C-176 was administered once daily from day 7 to day 11, the behavioral tests were also performed at 1h after C-176 injection from day 7 to day 11. Surprisingly, mechanical hypersensitivity and thermal allodynia was only transiently reversed at day 7 and day 8 but then decreased to a comparable level as those SNI group (Fig. 8D, Supplementary Figure S1D). For prevent treatment, C-176 (40 μg) was given 5 min before SNI surgery and day 1 after SNI surgery, results showed that the development of PWT and TWL were significantly delayed but not reversed following SNI (Fig. 8E, Supplementary Figure S1E). C-176 did not alter the PWT and TWL in sham mice or cause any obvious adverse effects (Fig. 8A-D, Supplementary Figure S1A-D). No significant difference in open field test was observed in mice that injected C-176 after SNI surgery when compared with mice in other group (Supplementary Figure S1F and G), suggesting overall locomotor activity was not influenced by C-176. Taken together, these results suggested that STING is critical during the initiation of pain hypersensitivity following SNI, but are only transiently required in the maintenance of neuropathic pain.

Early C-176 administration attenuated microglia activation and suppressed proinflammatory responses in the spinal cord after SNI.

Activation of STING signaling pathway was assessed by detecting the level of p-TBK1 and p-p65 in the L4-5 spinal cord dorsal horn. Data showed that the expression of STING, p-TBK1 and p-p65 was inhibited by repetitive injection of C-176 in the L4-5 spinal cord dorsal horn (Fig. 9A-C). NF-κB has long been defined a central regulator of inflammation, primarily in response to proinflammatory cytokines such as IL-1β, IL-6 and TNF-α [35]. To elucidate the exact mechanism of STING participating in pain, microglia activation and pro-inflammatory cytokines were assessed in SNI-injured pain model. The upregulation of microglia activation marker Iba1 following SNI was significantly reduced by repetitive injection of C-176 in the spinal cord dorsal horn at day 7 (Fig. 9D). Meanwhile, results showed that both downstream effectors of NF-κB and expression of M1 pro-inflammatory cytokines (iNOS, CD86, CD68 in protein, MCP-1, IL-1β, and TNF- α in mRNA, and IL-6 in Elisa) were significantly increased after SNI, repetitive injection of C-176 also significantly reduced the release of M1 pro-inflammatory responses, all of which were contribute to pain hypersensitivity (Fig. 9E-K) [36, 37]. These results illustrated that STING-TBK1-NF-κB activation and subsequent proinflammatory cytokines expression upregulation could promote spinal cord microglia activation and induce pain hypersensitivity.

Early C-176 administration attenuates pain hypersensitivity through IL-6/JAK2/STAT3 signaling in the spinal cord after SNI.

Previous studies show that IL-6 mainly activates JAK/STAT signaling pathway in spinal microglia and contributes to neuropathic pain in nerve injury model [32, 33]. Thus, the possible role of IL-6 in the activation of the JAK2/STAT3 pathway was assessed in the spinal cord following SNI. Western blot analysis showed that the expression of phosphorylated JAK2 and STAT3 was significantly increased at day 1, peaked at day 3 following SNI (Fig. 10A) and C-176 could significantly inhibited this upregulation (Fig. 10B). To further evaluate whether IL-6/JAK2/STAT3 was involved in the analgesic effect of STING in SNI mice, mice recombinant of IL-6 (rIL-6) was given intrathecal together with C-176, PWT and TWL were

evaluated on day 7 after surgery. Data showed mice treated with rIL-6 alone showed significantly decrease in PWT and TWL, illustrating that IL-6 plays a role in the development of neuropathic pain. However, the analgesic effects of C-176 were largely abolished by rIL-6 injection (Fig. 10C), suggesting that C-176 exhibited its analgesic effect by IL-6 inhibition.

Moreover, rIL-6 injection almost completely reversed the downregulated expression of phosphorylated JAK2 and STAT3 in the spinal cord of SNI mice (Fig. 10D). Our pervious study has already demonstrated that JAK2/STAT3 was mainly colocalized to microglia in the nociceptive pathway [38]. Furthermore, we assessed the effects of STING on activation of JAK2/STAT3 using BV-2 cells, demonstrating that STING activation could increase the phosphorylation level of JAK2/STAT3 signal in microglia. These results revealed that STING mediated SNI-induced neuropathic pain via IL-6/JAK2/STAT3 in the spinal cord microglia.

Discussion

Emerging evidence suggested that the neuroimmune response plays a critical role in the generation of neuropathic pain [14], however, the precise mechanisms were largely unknown. A previous study has suggested that intrathecal intracellular dsDNA could exhibit IFN-I-dependent antinociception in naïve mice [34]. In our study, we found that dsDNA in the peripheral blood was significantly increased following SNI and the increased self-DNA plays a critical role for activating STING and promoting inflammation following SNI. Thus, we supposed that STING may play a pivotal role in neuropathic pain through sensing the increased self-dsDNA. However, the source of the upregulated circulating dsDNA and the precise mechanisms underlying dsDNA-induced signaling transduction in the spinal cord following SNI is unclear.

As we know, nerve injury could induce dying/dead or injured cells releasing large amounts of DNA into the extracellular environment via necrosis or apoptosis [39, 40]. Normally, this self-DNA is normally nonimmunogenic. However, our understanding has since developed, emerging studies demonstrated that extracellular self-dsDNA can get access to the cytosol through Fc receptors [41]. It also has been proposed that extracellular self-dsDNA can be transferred into monocytes by an endogenous antimicrobial peptide LL37 [42, 43]. Moreover, additional DNA receptors may exist in the cytoplasm in macrophages for detecting DNA [44]. In addition, mitochondrial DNA (mtDNA) is another main source of DNA for STING activating [45, 46] and several possible mechanisms has been proposed. For example, the release of mtDNA could be triggered by BCL-2-like protein 4 (BAX)- and BCL-2 homologous killer (BAK)-mediated apoptosis [47], activation of mitochondrial permeability transition pore [48], deficiency of transcription factor A mitochondrial (TFAM) or aberrant mtDNA packaging [49]. Though the mechanisms have been explored widely, further studies are still needed to identify the source and localization of dsDNA considering dsDNA sensor and dsDNA sensing might be different.

It has been proved that dsDNA play an integral role in STING pathway activation [50]. Once STING has been activated, STING then recruits kinases such as TBK1, and phosphorylated both the interferons (IFN)

regulatory factor 3 (IRF3) and NF-κB by TBK1. P-IRF3 subsequently enters the nucleus and ultimately upregulating the expression of type I IFN (IFN-I) and mediates innate immune response, and p-p65 could promote the expression of proinflammatory cytokines (such as IL-1β, IL-6 and TNF-α) that facilitate inflammation and immunity [6, 9, 51, 52]. In our study, STING was activated after sensing dsDNA in spinal cord microglia after SNI. Though we cannot rule out the effect of STING in other cell types, immunofluorescence result has demonstrated STING was mostly colocalized to Iba1 microglia. To assess the role of STING in microglia, DMXAA was used in BV-2 cells. As expected, DMXAA treatment significantly activated STING/TBK1/NF-κB pathway, and increased the production of proinflammatory cytokines and chemokines (such as iNOS, MCP-1, IL-1β, IL-6 and TNF-α), as well as phosphorylated JAK2/STAT3 signal in BV-2 cells.

Recent studies indicated that activation of STING could promote microglial activation in several inflammatory models [53–55].The role of microglial activation in the development of SNI-induced neuropathic pain was corroborated by several pieces of evidence [30, 56]. In our effort to clarify the mechanisms underlying microglia activation, we found that microglia and microglial response (including morphological change, proliferation, and release of mediators such as IL-1β, IL-6 and TNF-α) are essential for the induction of neuropathic pain after peripheral nerve injury [31]. A recent study has supposed that STING play a critical role for chronic pain status [34]. However, our study emphasizes the role of STING in spinal cord microglia in the induction of pain hypersensitivity. Consistent with the temporal patterns of microglia, the expression level of STING/ TBK1/NF-κB and its downstream effectors were significantly upregulated at an early time with peaks between day 3 to day 7, and early but not late STING inhibitor C-176 could significantly inhibit STING signaling pathway and attenuate mechanical allodynia and thermal hyperalgesia in SNI mice. These results suggested that microglial STING may be the basis of the temporal role of microglia in the initiation, but is not essential for maintenance of neuropathic pain. It is noteworthy to mention that Donnelly et al. [34] reported that the STING could regulate chronic pain and steady-state nociception, which was involved in IFN-I signaling. However, in our study, IFN-β, a key component of type I IFN, was not significantly increased until day 14, thus it seems to play a dominant role in the maintaining of pathological pain states. This discrepancy may be involved in different doses of administration, injection time and experimental animals. Given together, we hypothesized that STING/TBK1/NF-κB may play a dominant role in the initiation of neuropathic pain [34].

IL-6, as a mediator for pathological pain management [57], patch-clamp recordings of isolated spinal cord slices suggested that IL-6 could reduce the frequency of spontaneous inhibitory postsynaptic currents [36]. IL-6 can be produced at the site of peripheral nerve injury and also produced centrally for the response to nerve injury. Recombinant human IL-6 injection could exacerbate pain behaviors in a neuropathic pain model [58] and anti-IL-6 neutralizing antibody injection could alleviate these pain-related behaviors [57]. Moreover, it has been proved that endogenous IL-6 displayed an important early role for glial activation in the spinal cord following nerve injury [58]. Our findings suggested that spinal cord microglia and microglial STING signaling could be activated following SNI and both could contribute to upregulation of IL-6, demonstrating a critical role of IL-6 following SNI. Dominguez et al [59, 60] proposed that IL-6 may act as an important early signal through activation of JAK/STAT after combining with IL-6

receptor following nerve injury. In our study, p-JAK2 increased at day 1 and peaked at day 3 following SNI, while p-STAT3 increased at day 1 and maintained at a high level until day 14. Our previous study and others has already illustrated that JAK2/STAT3 signal was mainly colocalized to microglia in the spinal cord [38, 60]. Based on these data, we propose that STING could regulate IL-6/JAK2/STAT3 axis for pain management in the spinal cord microglia. We further confirmed this conclusion in mice treatment with rIL-6, the results showed that injection of rIL-6 intrathecally significantly increased the pain hypersensitivity and p-JAK2/STAT3 generation after SNI. These results suggested that STING exerts its biological effect in SNI-induced pain hypersensitivity, at least partly via IL-6/JAK2/STAT3 signaling in the spinal cord microglia (Fig. 11). And pharmacological inhibition of STING may be an effective way for early intervention of pain development.

Conclusion

In conclusion, our study identified that microglial STING acted as an early critical mediator for dsDNA sensing and proinflammatory cytokines releasing in the spinal cord, played a critical role in the development of neuropathic pain. Moreover, our results indicated that STING contributed to SNI-induced pain hypersensitivity by promoting microglia polarization to M1 phenotype and exacerbating releasing of proinflammatory factors in the spinal cord dorsal horn. Pharmacological blockade of STING had important therapeutic implications by inhibiting IL-6/JAK2/STAT3 axis after SNI. In summary, targeting STING may be novel and promising therapeutic implications for early intervention of pain development.

Abbreviations

BAK: BCL-2 homologous killer; BAX: BCL-2-like protein 4; cGAS: cyclic GMP-AMP synthase; DMEM: Dulbecco's modified Eagles medium; DMSO: Dimethyl sulfoxide dsDNA: double-stranded DNA; ELISA: Enzyme-linked immunosorbent assay; ER: endoplasmic reticulum; GFAP: Glial fibrillary acidic protein; HRP: Horseradish peroxidase; Iba1: Ionized calcium-binding adapter molecule 1; IF: Immunofluorescence; IFNs: interferons; IL-1β, interleukin 1β; IL-6, interleukin 6; iNOS, inducible nitric oxide synthase; IRF3: interferons regulatory factor 3; JAK: Janus-activated kinase; MCP-1: monocyte chemotactic protein 1; mtDNA, mitochondrial DNA; NeuN: Neuronal nuclei; NF-κB, nuclear factor-kappa B; OFM: open Field Maze; PAMPs: pathogen-associated molecular patterns; PBS: Phosphate buffered saline; PCR: Polymerase Chain Reaction; PFA: Paraformaldehyde; PWT, paw withdrawal threshold; RT: room temperature; SNI: spared nerve injury; STAT3: signal transducer activator of transcription 3; STING, stimulator of interferon genes; TBK1, TANK-binding kinase 1; TNF-α, tumor necrosis factor-α; TFAM, transcription factor A, mitochondrial; TWL, thermal withdrawal latency; WB: Western blot

Declarations

Acknowledgements

We thank Prof. Pei-Xiang Lan for helpful guidance and discussions.

Authors' contributions

WM, DWY and YQZ conceived the project and supervised all experiments. JS and BYX analyzed data, prepared figures and wrote manuscripts. JS, JYL, LQZ, JYW and SJG performed experiments on behavioral tests, western blot, ELISA, and immunofluorescence. and HD, YC, and HZ performed experiments and analyzed data. WM, DQL and PXL revised manuscript. All authors read and approved the final manuscript.

Funding

This work was supported by grants from National Natural Science Foundation of P.R. China 82071556 and 81873793.

Availability of data and materials

The data and materials supporting the conclusions of this study are available from the corresponding author on reasonable request.

Ethics approval and consent to participate

All experiments were approved by the Experimental Animal Care and Use Committee of Tongji Medical College, Huazhong University of Science and Technology, and were in agreement with the National Institutes of Health Guidelines for the Care and Use of Laboratory Animals.

Consent for publication

Not applicable.

Competing interests

The authors have no conflicts of interest to declare.

Author details

1. Anesthesiology Institute, Tongji Hospital, Tongji Medical College, Huazhong University of Science and Technology, Wuhan, China.
2. Department of Anesthesiology and Pain Medicine, Tongji Hospital, Tongji Medical College, Huazhong University of Science and Technology, Wuhan, China.
3. Institute of Organ Transplantation, Tongji Hospital, Tongji Medical College, Huazhong University of Science and Technology, Key Laboratory of Organ Transplantation, Ministry of Education, NHC Key Laboratory of Organ Transplantation, Key Laboratory of Organ Transplantation, Chinese Academy of Medical Sciences, Wuhan, China
4. Cancer Center, Tongji Hospital, Tongji Medical college, Huazhong University of Science and Technology, Wuhan, China.

References

1. Jensen TS, Baron R, Haanp?? M, Kalso E, Loeser JD, Rice ASC, Treede RD: **A new definition of neuropathic pain.***Pain* 2011, **152:**2204-2205.
2. Palm NW, Medzhitov R: **Pattern recognition receptors and control of adaptive immunity.***Immunological Reviews* 2010, **227:**221-233.
3. Beutler B: **Microbe sensing, positive feedback loops, and the pathogenesis of inflammatory diseases.***Immunological Reviews* 2009, **227**.
4. Kawai T, Akira S: **The roles of TLRs, RLRs and NLRs in pathogen recognition.***International Immunology* 2009.
5. Palm NW, Medzhitov R: **Palm, N. W. & Medzhitov, R. Pattern recognition receptors and control of adaptive immunity. Immunol. Rev. 227, 221-233.***Immunological Reviews* 2009, **227:**221-233.
6. Luo W, Wang Y, Zhang L, Ren P, Shen YH: **Critical Role of Cytosolic DNA and Its Sensing Adaptor STING in Aortic Degeneration, Dissection, and Rupture.***Circulation* 2020, **141:**42-66.
7. Zhu Y, An X, Zhang X, Qiao Y, Zheng T, Li X: **STING: a master regulator in the cancer-immunity cycle.***Mol Cancer* 2019, **18:**152.
8. Saitoh T, Fujita N, Hayashi T, Takahara K, Satoh T, Lee H, Matsunaga K, Kageyama S, Omori H, Noda T, et al: **Atg9a controls dsDNA-driven dynamic translocation of STING and the innate immune response.***Proc Natl Acad Sci U S A* 2009, **106:**20842-20846.
9. Jeonghyun, Ahn, Gutman, Delia, Saijo, Shinobu, Barber, Glen, N.: **STING manifests self DNA-dependent inflammatory disease.***Proceedings of the National Academy of Sciences of the United States of America* 2012.
10. Li N, Zhou H, Wu H, Wu Q, Duan M, Deng W, Tang Q: **STING-IRF3 contributes to lipopolysaccharide-induced cardiac dysfunction, inflammation, apoptosis and pyroptosis by activating NLRP3.***Redox Biol* 2019, **24:**101215.
11. Sliter DA, Martinez J, Hao L, Chen X, Sun N, Fischer TD, Burman JL, Li Y, Zhang Z, Narendra DP, et al: **Parkin and PINK1 mitigate STING-induced inflammation.***Nature* 2018, **561:**258-262.
12. Abdullah A, Zhang M, Frugier T, Bedoui S, Taylor JM, Crack PJ: **STING-mediated type-I interferons contribute to the neuroinflammatory process and detrimental effects following traumatic brain injury.***J Neuroinflammation* 2018, **15:**323.
13. Sommer C, Leinders M, Uceyler N: **Inflammation in the pathophysiology of neuropathic pain.***Pain* 2018, **159:**595-602.
14. A MC, A JMD, B DDLBA: **The role of the immune system in the generation of neuropathic pain - ScienceDirect.***Lancet Neurology* 2012, **11:**629-642.
15. Pankaj, Baral, Swalpa, Udit, Isaac, Chiu: **Pain and immunity: implications for host defence.***Nature Reviews Immunology* 2019.
16. Pinho-Ribeiro FA, Verri WA, Chiu IM: **Nociceptor Sensory Neuron–Immune Interactions in Pain and Inflammation.***Trends in Immunology* 2016**:**5.

17. Cao F, Gao F, Xu AJ, Chen ZJ, Chen SS, Yang H, Yu HH, Mei W, Liu XJ, Xiao XP, et al: **Regulation of spinal neuroimmune responses by prolonged morphine treatment in a rat model of cancer induced bone pain.***Brain Res* 2010, **1326:**162-173.
18. Grace PM, Rolan PE, Hutchinson MR: **Peripheral immune contributions to the maintenance of central glial activation underlying neuropathic pain.***Brain Behavior and Immunity* 2011, **25:**1322-1332.
19. Block ML, Zecca L, Hong JS: **Microglia-mediated neurotoxicity: uncovering the molecular mechanisms.***Nature Reviews Neuroscience* 2007, **8:**57-69.
20. Chen G, Zhang YQ, Qadri YJ, Serhan CN, Ji RR: **Microglia in Pain: Detrimental and Protective Roles in Pathogenesis and Resolution of Pain.***Neuron* 2018, **100:**1292-1311.
21. Kobayashi K, Imagama S, Ohgomori T, Hirano K, Uchimura K, Sakamoto K, Hirakawa A, Takeuchi H, Suzumura A, Ishiguro N, Kadomatsu K: **Minocycline selectively inhibits M1 polarization of microglia.***Cell Death Dis* 2013, **4:**e525.
22. Le WD, Rowe D, Xie WJ, Ortiz I, Appel SH: **Microglial Activation and Dopaminergic Cell Injury: An In Vitro Model Relevant to Parkinson's Disease.***The Journal of Neuroence : The Official Journal of the Society for Neuroence* 2001, **21:**8447-8455.
23. Li Z, Wei H, Piirainen S, Chen Z, Kalso E, Pertovaara A, Tian L: **Spinal versus brain microglial and macrophage activation traits determine the differential neuroinflammatory responses and analgesic effect of minocycline in chronic neuropathic pain.***Brain Behav Immun* 2016, **58:**107-117.
24. Ann KK, Byrnes KR, Grunberg NE, Kasper CE, Lisa O, Brian P, Tosini NL, Xingjia W, Anders JJ: **Characterization of Macrophage/Microglial Activation and Effect of Photobiomodulation in the Spared Nerve Injury Model of Neuropathic Pain.***Pain Medicine***:**932.
25. Burke NN, Kerr DM, Moriarty O, Finn DP, Roche M: **Minocycline modulates neuropathic pain behaviour and cortical M1-M2 microglial gene expression in a rat model of depression.***Brain Behav Immun* 2014, **42:**147-156.
26. Honjoh K, Nakajima H, Hirai T, Watanabe S, Matsumine A: **Relationship of Inflammatory Cytokines From M1-Type Microglia/Macrophages at the Injured Site and Lumbar Enlargement With Neuropathic Pain After Spinal Cord Injury in the CCL21 Knockout (plt) Mouse.***Front Cell Neurosci* 2019, **13:**525.
27. Zhou YQ, Liu DQ, Chen SP, Chen N, Sun J, Wang XM, Cao F, Tian YK, Ye DW: **Nrf2 activation ameliorates mechanical allodynia in paclitaxel-induced neuropathic pain.***Acta Pharmacol Sin* 2020.
28. Zhou YQ, Liu DQ, Chen SP, Sun J, Zhou XR, Rittner H, Mei W, Tian YK, Zhang HX, Chen F, Ye DW: **Reactive oxygen species scavengers ameliorate mechanical allodynia in a rat model of cancer-induced bone pain.***Redox Biol* 2018, **14:**391-397.
29. Deng L, Liang H, Xu M, Yang X, Burnette B, Arina A, Li XD, Mauceri H, Beckett M, Darga T, et al: **STING-Dependent Cytosolic DNA Sensing Promotes Radiation-Induced Type I Interferon-Dependent Antitumor Immunity in Immunogenic Tumors.***Immunity* 2014, **41:**843-852.
30. Watkins LR, Milligan ED, Maier SF: **Glial activation: a driving force for pathological pain.***Trends in Neurosciences* 2001, **24:**450-455.

31. Kim D, You B, Jo EK, Han SK, Simon MI, Lee SJ: **NADPH oxidase 2-derived reactive oxygen species in spinal cord microglia contribute to peripheral nerve injury-induced neuropathic pain.***Proc Natl Acad Sci U S A* 2010, **107:**14851-14856.
32. Dominguez, Elisa, Mauborgne, Annie, Mallet, Jacques, Desclaux, Mathieu, Pohl, Michel: **SOCS3-Mediated Blockade of JAK/STAT3 Signaling Pathway Reveals Its Major Contribution to Spinal Cord Neuroinflammation and Mechanical Allodynia after Peripheral Nerve Injury.***Journal of Neuroscience* 2010.
33. Dominguez E, Rivat C, Pommier B, Mauborgne A, Pohl M: **JAK/STAT3 pathway is activated in spinal cord microglia after peripheral nerve injury and contributes to neuropathic pain development in rat.***J Neurochem* 2008, **107:**50-60.
34. Donnelly CR, Jiang C, Andriessen AS, Wang K, Wang Z, Ding H, Zhao J, Luo X, Lee MS, Lei YL, et al: **STING controls nociception via type I interferon signalling in sensory neurons.***Nature* 2021.
35. Robinson SM, Mann DA: **Role of nuclear factor κB in liver health and disease.***Clinical Science* 2010, **118:**691-705.
36. Kawasaki Y, Zhang L, Cheng JK, Ji RR: **Cytokine mechanisms of central sensitization: distinct and overlapping role of interleukin-1beta, interleukin-6, and tumor necrosis factor-alpha in regulating synaptic and neuronal activity in the superficial spinal cord.***Journal of Neuroscience* 2008, **28:**5189-5194.
37. Van Steenwinckel J, Reaux-Le Goazigo A, Pommier B, Mauborgne A, Dansereau MA, Kitabgi P, Sarret P, Pohl M, Melik Parsadaniantz S: **CCL2 released from neuronal synaptic vesicles in the spinal cord is a major mediator of local inflammation and pain after peripheral nerve injury.***J Neurosci* 2011, **31:**5865-5875.
38. Chen SP, Sun J, Zhou YQ, Cao F, Braun C, Luo F, Ye DW, Tian YK: **Sinomenine attenuates cancer-induced bone pain via suppressing microglial JAK2/STAT3 and neuronal CAMKII/CREB cascades in rat models.***Mol Pain* 2018, **14:**1744806918793232.
39. Barker RN, Erwig LP, Pearce WP, Devine A, Rees AJ: **Differential Effects of Necrotic or Apoptotic Cell Uptake on Antigen Presentation by Macrophages.***Pathobiology* 1999, **67:**302-305.
40. Sauter B, Albert ML, Francisco L, Larsson M, Somersan S, Bhardwaj N: **Consequences of cell death: exposure to necrotic tumor cells, but not primary tissue cells or apoptotic cells, induces the maturation of immunostimulatory dendritic cells.***J Exp Med* 2000, **191:**423-434.
41. Bauer, Stefan: **Toll-erating self DNA.***Nature Immunology* 2006, **7:**13-15.
42. Chamilos G, Gregorio J, Meller S, Lande R, Kontoyiannis DP, Modlin RL, Gilliet M: **Cytosolic sensing of extracellular self-DNA transported into monocytes by the antimicrobial peptide LL37.***Blood* 2012, **120:**3699.
43. Zhao Q, Wei Y, Pandol SJ, Li L, Habtezion A: **STING Signaling Promotes Inflammation in Experimental AcutePancreatitis.***Gastroenterology* 2018**:**1822-1835.
44. Hornung V, Latz E: **Intracellular DNA recognition.***Nat Rev Immunol* 2010, **10:**123-130.

45. West AP, Shadel GS: **Mitochondrial DNA in innate immune responses and inflammatory pathology.***Nature Reviews Immunology* 2017.
46. Burdette DL, Vance RE: **STING and the innate immune response to nucleic acids in the cytosol.***Nat Immunol* 2013, **14:**19-26.
47. White MJ, McArthur K, Metcalf D, Lane RM, Cambier JC, Herold MJ, van Delft MF, Bedoui S, Lessene G, Ritchie ME, et al: **Apoptotic caspases suppress mtDNA-induced STING-mediated type I IFN production.***Cell* 2014, **159:**1549-1562.
48. Patrushev M, Kasymov V, Patrusheva V, Ushakova T, Gogvadze V, Gaziev A: **Mitochondrial permeability transition triggers the release of mtDNA fragments.***Cellular & Molecular Life Sciences Cmls* 2004, **61:**3100-3103.
49. West AP, Khoury-Hanold W, Staron M, Tal MC, Pineda CM, Lang SM, Bestwick M, Duguay BA, Raimundo N, MacDuff DA, et al: **Mitochondrial DNA stress primes the antiviral innate immune response.***Nature* 2015, **520:**553-557.
50. Benmerzoug S, Rose S, Bounab B, Gosset D, Duneau L, Chenuet P, Mollet L, Le Bert M, Lambers C, Geleff S, et al: **STING-dependent sensing of self-DNA drives silica-induced lung inflammation.***Nat Commun* 2018, **9:**5226.
51. Li T, Chen ZJ: **The cGAS-cGAMP-STING pathway connects DNA damage to inflammation, senescence, and cancer.***J Exp Med* 2018, **215:**1287-1299.
52. Chen Q, Sun L, Chen ZJ: **Regulation and function of the cGAS-STING pathway of cytosolic DNA sensing.***Nat Immunol* 2016, **17:**1142-1149.
53. Peng Y, Zhuang J, Ying G, Zeng H, Zhou H, Cao Y, Chen H, Xu C, Fu X, Xu H, et al: **Stimulator of IFN genes mediates neuroinflammatory injury by suppressing AMPK signal in experimental subarachnoid hemorrhage.***J Neuroinflammation* 2020, **17:**165.
54. Chang HH, Miaw SC, Tseng W, Sun YW, Liu CC, Tsao HW, Ho IC: **PTPN22 Modulates Macrophage Polarization and Susceptibility to Dextran Sulfate Sodium-Induced Colitis.***Journal of Immunology* 2013.
55. Hunter MM, Wang A, Parhar KS, Johnston MJG, Rooijen NV, Beck PL, Mckay DM: **In Vitro-Derived Alternatively Activated Macrophages Reduce Colonic Inflammation in Mice.***Gastroenterology* 2010, **138:**1395-1405.
56. Inoue K, Tsuda M: **Microglia in neuropathic pain: cellular and molecular mechanisms and therapeutic potential.***Nat Rev Neurosci* 2018, **19:**138-152.
57. Zhou YQ, Liu Z, Liu ZH, Chen SP, Li M, Shahveranov A, Ye DW, Tian YK: **Interleukin-6: an emerging regulator of pathological pain.***J Neuroinflammation* 2016, **13:**141.
58. Deleo JA, Colburn RW, Nichols M, Malhotra A: **Interleukin-6-mediated hyperalgesia/allodynia and increased spinal IL-6 expression in a rat mononeuropathy model.***Journal of Interferon & Cytokine Research the Official Journal of the International Society for Interferon & Cytokine Research* 1996, **16:**695-700.

59. Dominguez E, Mauborgne A, Mallet J, Desclaux M, Pohl M: **SOCS3-mediated blockade of JAK/STAT3 signaling pathway reveals its major contribution to spinal cord neuroinflammation and mechanical allodynia after peripheral nerve injury.***Journal of Neuroscience the Official Journal of the Society for Neuroscience* 2010, **30:**5754.
60. Dominguez E, Rivat C, Pommier B, Mauborgne A, Pohl M: **JAK/STAT3 pathway is activated in spinal cord microglia after peripheral nerve injury and contributes to neuropathic pain development in rat.***Journal of Neurochemistry* 2008, **107:**50-60.

Figures

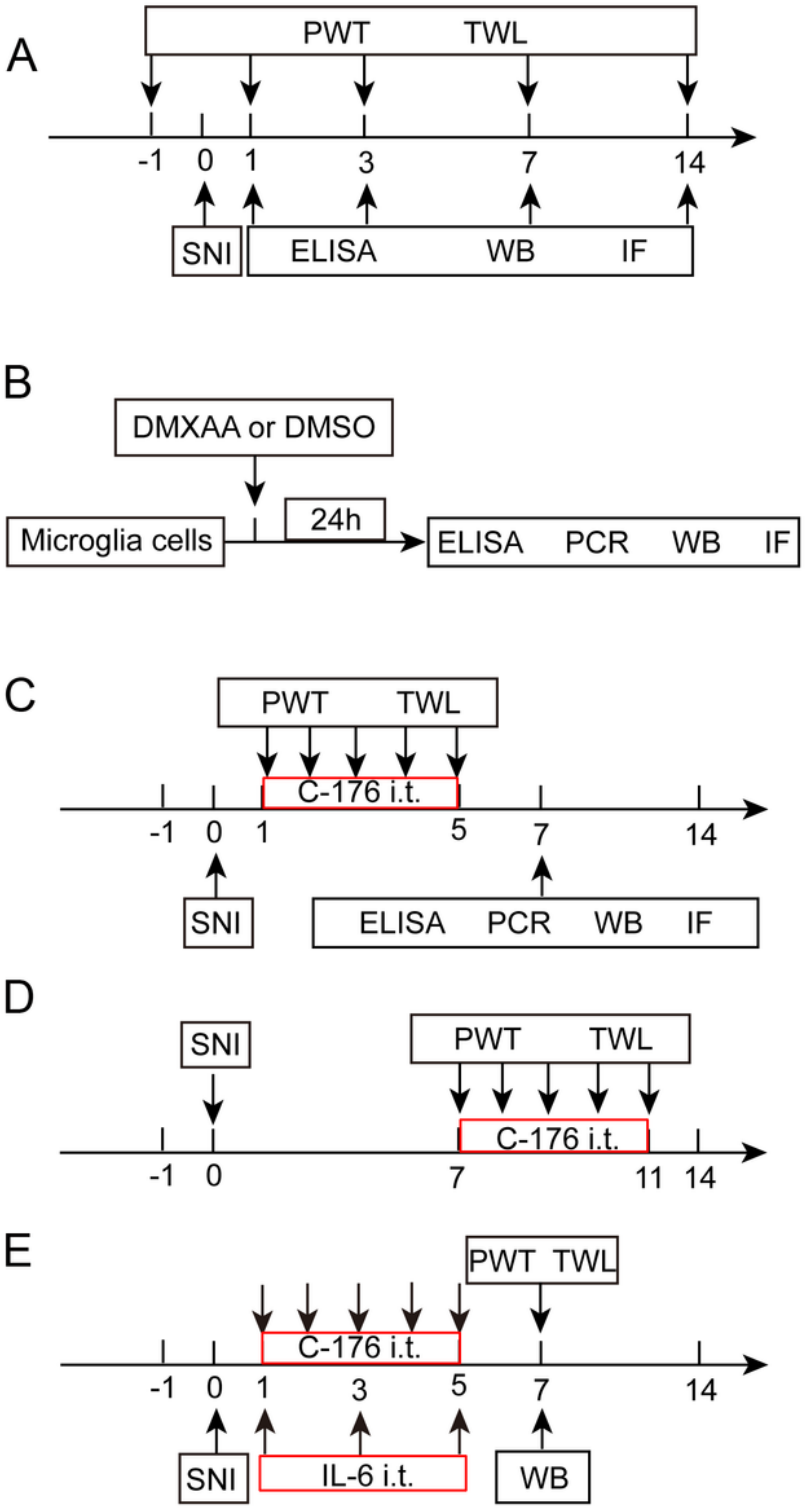

Figure 1

Experimental designs animal groups. (A) Time course of pain behaviors and pro-inflammatory cytokines in the spinal cord following SNI. (B) The effects of DMXAA on microglia cells. (C) Effects of early treatment of C-176 on pain hyperintensity, STING signaling pathway and its downstream effectors following SNI. (D) Effects of late treatment of C-176 on pain hyperintensity. (E) Effects of mice rIL-6 in the analgesic effect of C-176. ELISA: enzyme-linked immunosorbent assay; IF: immunofluorescence; PCR:

Polymerase Chain Reaction; PWT: paw withdrawal threshold; TWL: thermal withdrawal latency; WB: western blot

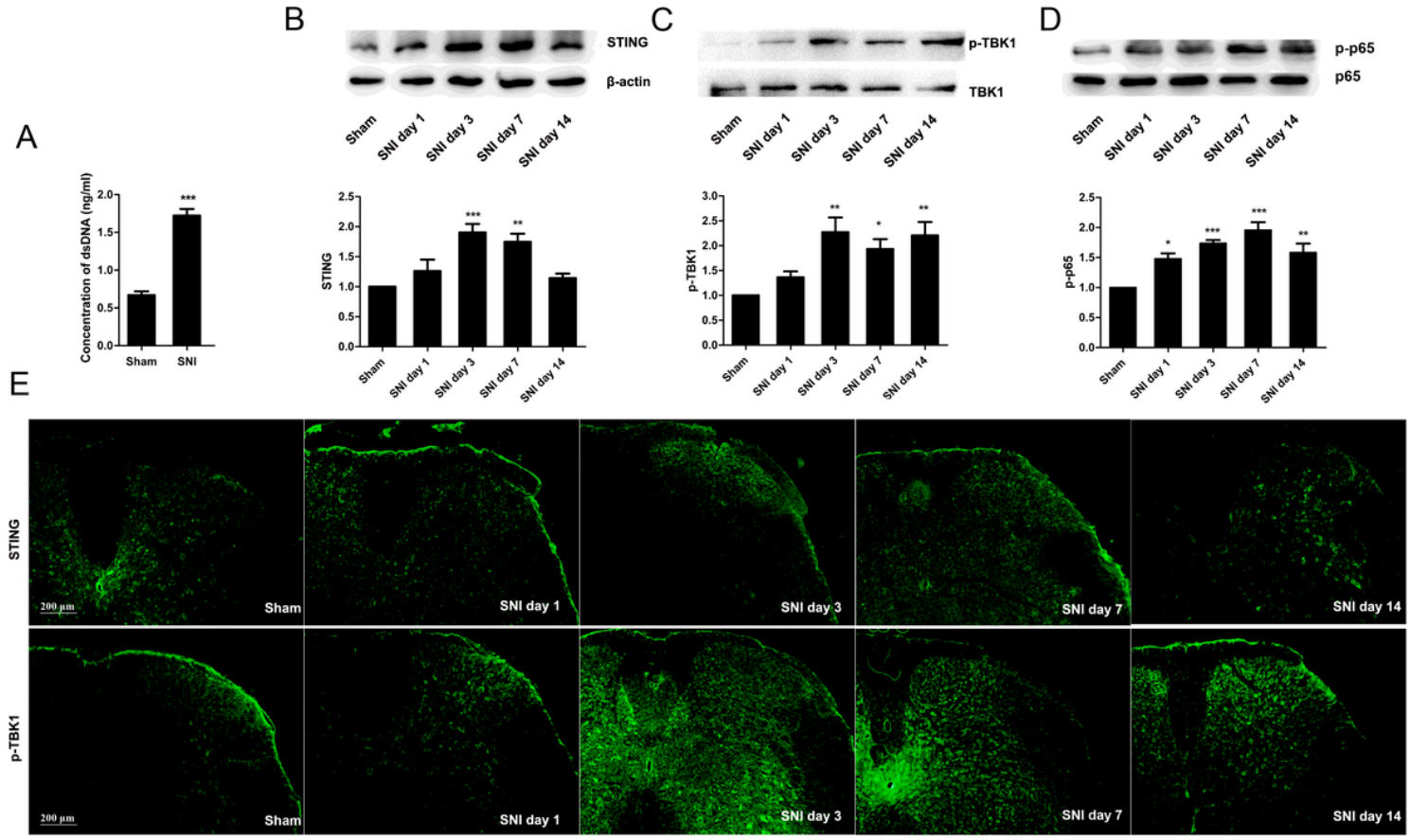

Figure 2

SNI increased the level of dsDNA and activated STING signaling pathway. (A) Elisa analysis showed the level of dsDNA in the peripheral blood was significantly upregulated following SNI (n=3 per group). (B) The expression of STING in the L4-5 spinal cord was measured by western blotting at day 1, 3, 7, and 14 after SNI surgery (n=5 per group). (C) The expression of p-TBK1 in the L4-5 spinal cord was measured by western blotting at 1, 3, 7, and 14 d after SNI surgery (n=5 per group) (D) The expression of p-NF-κB p65 in the L4-5 spinal cord was measured by western blotting at 1, 3, 7, and 14 d after SNI surgery (n=5 per group). (E) The expression of STING and p-TBK1 in the L4-5 spinal cord was measured by immunostaining at 1, 3, 7, and 14 d after SNI surgery (n=3 per group, bar=200 μm). All data are presented as means ± SEM. (*P<0.05, **P<0.01, ***P<0.001 compared with the sham-operated group).

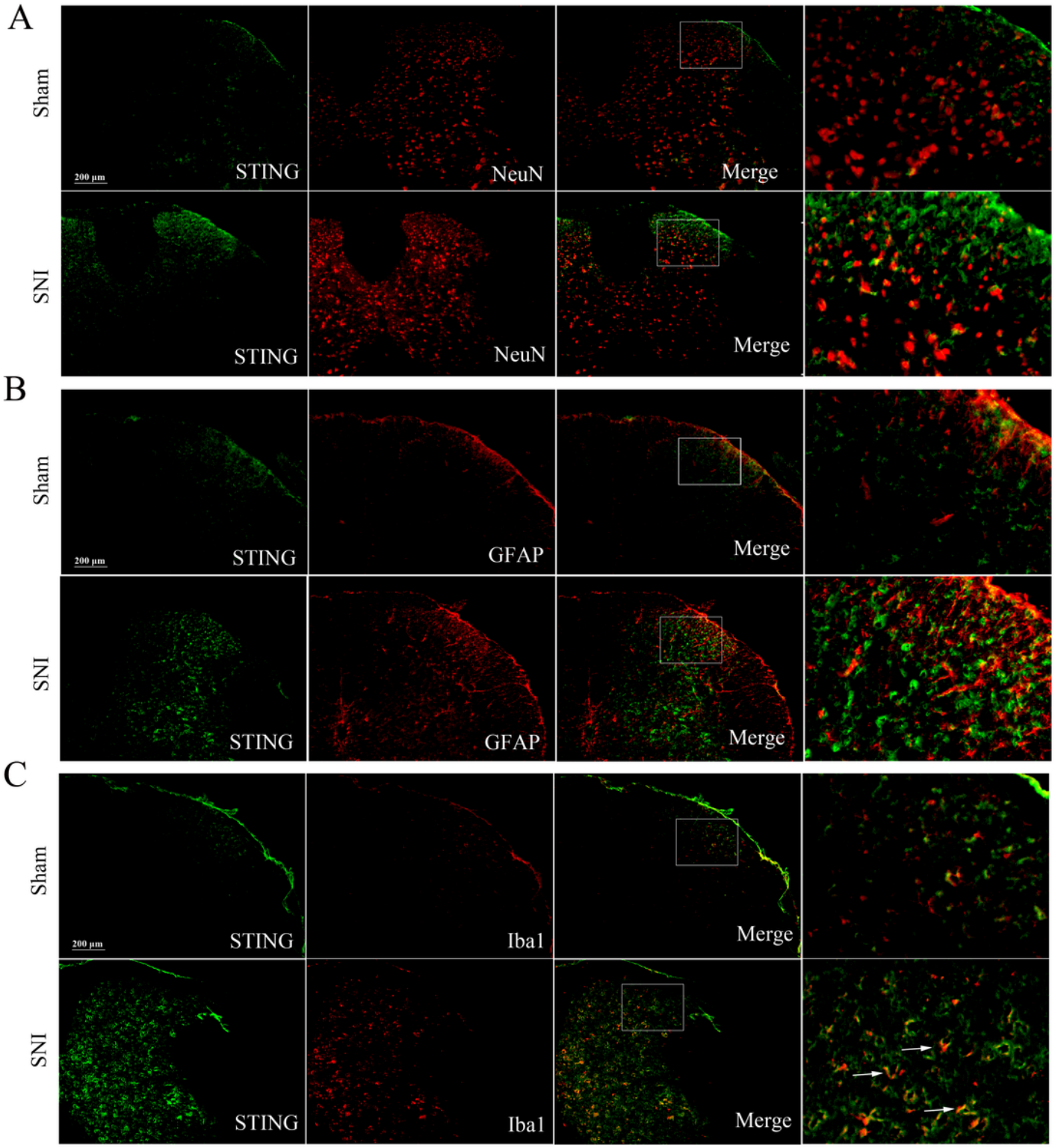

Figure 3

Expression and cellular localization of STING in spinal cord dorsal horn. (A-C) Representative images of STING double immunostained with neurons (NeuN), astrocyte (GFAP) and microglia (Iba1) in the spinal cord at day 7 following SNI. Immunofluorescence data showed that STING was increased in the spinal cord dorsal horn following SNI and STING was mainly colocalized with microglia in the spinal cord following SNI. Yellow represents colocalization (n=3 per group, bar=200 μm)

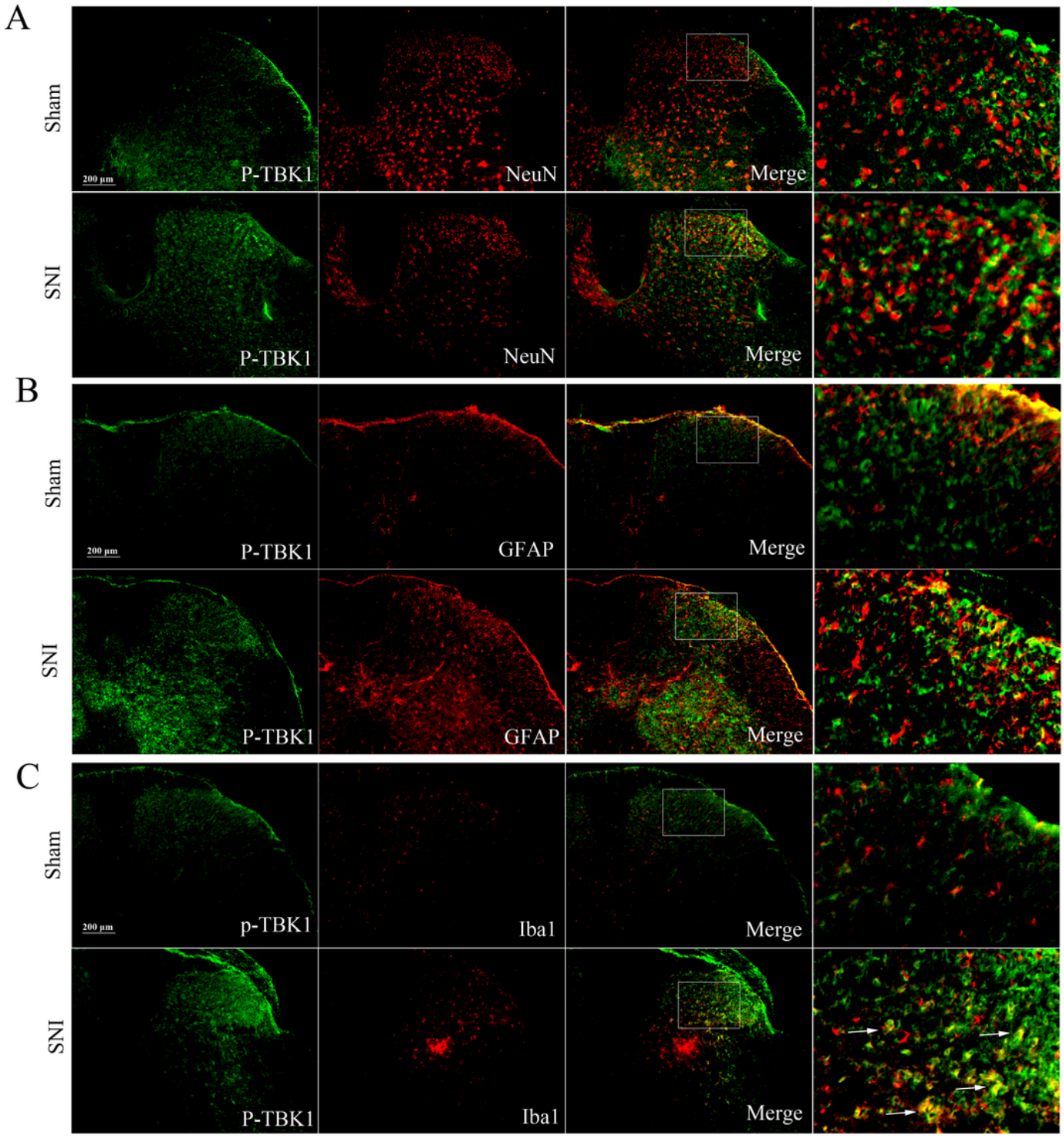

Figure 4

Expression and cellular localization of p-TBK1 in spinal cord dorsal horn. (A-C) Representative images of p-TBK1 double immunostained with neurons (NeuN), astrocyte (GFAP) and microglia (Iba1) in the spinal cord at day 7 after SNI. Immunofluorescence data showed that STING was upregulated in the spinal cord dorsal horn after SNI and STING was mainly colocalized with microglia in the spinal cord following SNI. Yellow represents colocalization (n=3 per group, bar=200 μm)

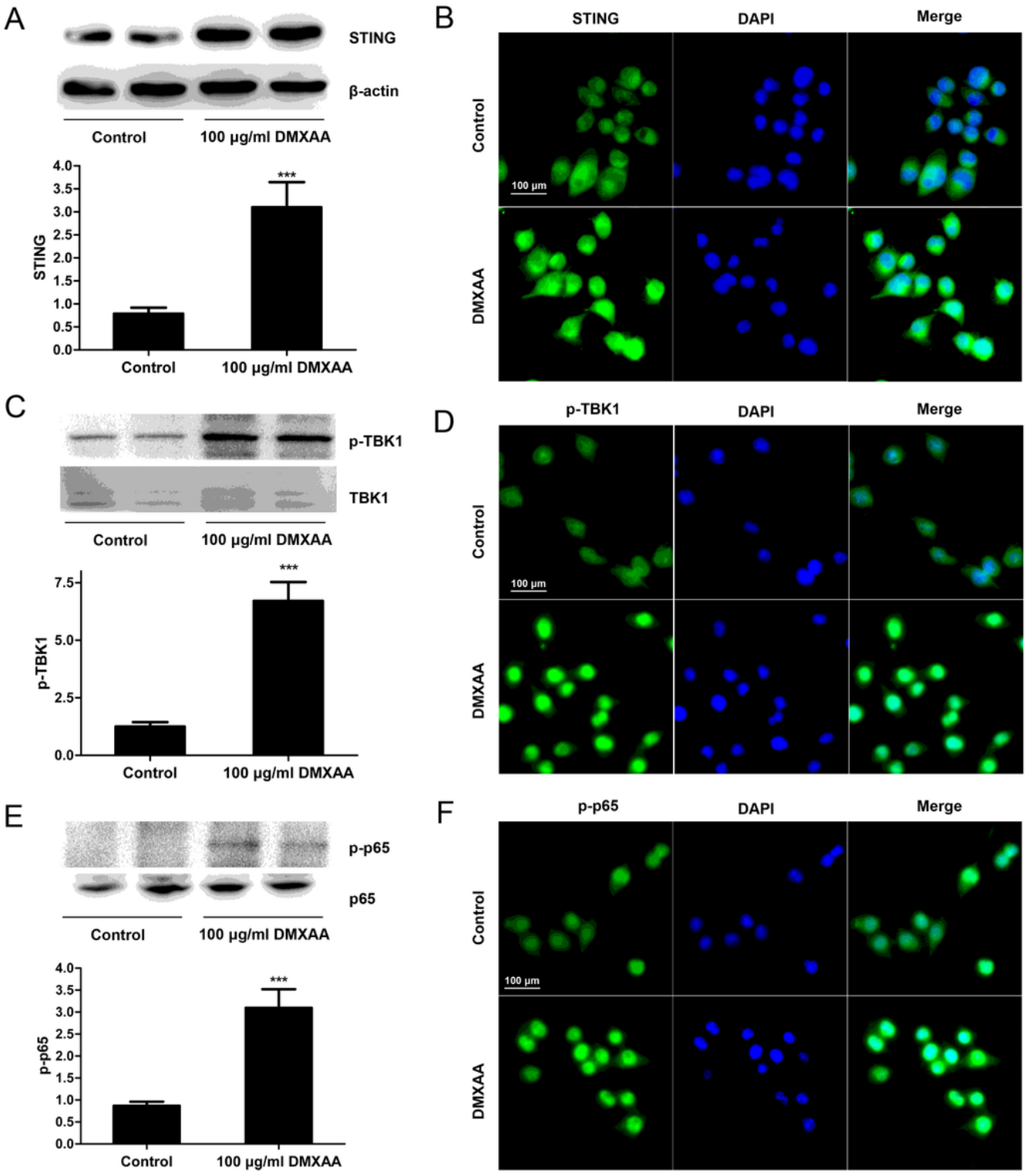

Figure 5

DMXAA activated STING signaling pathway and affected the intracellular location of STING, TBK1 and NF-κB. BV-2 cells were stimulated by DMXAA for 24 h. (A)The protein levels of STING in BV-2 cells stimulated by DMXAA for 24 h (n=4 per group). (B) Representative images of immunofluorescence of STING in BV-2 cells (n=3 per group, bar=100 μm). (C) The protein levels of p-TBK1 in BV-2 cells stimulated by DMXAA for 24 h (n=4 per group). (D) Representative images of immunofluorescence of p-

TBK1 in BV-2 cells (n=3 per group, bar=100 μm). (E)The protein levels of p-NF-κB p65 in BV-2 cells stimulated by DMXAA for 24 h (n=4 per group). (F) Representative images of immunofluorescence of p-NF-κB p65 in BV-2 cells (n=3 per group, bar=100 μm). All data are presented as means ± SEM. (***P<0.001 compared with the Control group)

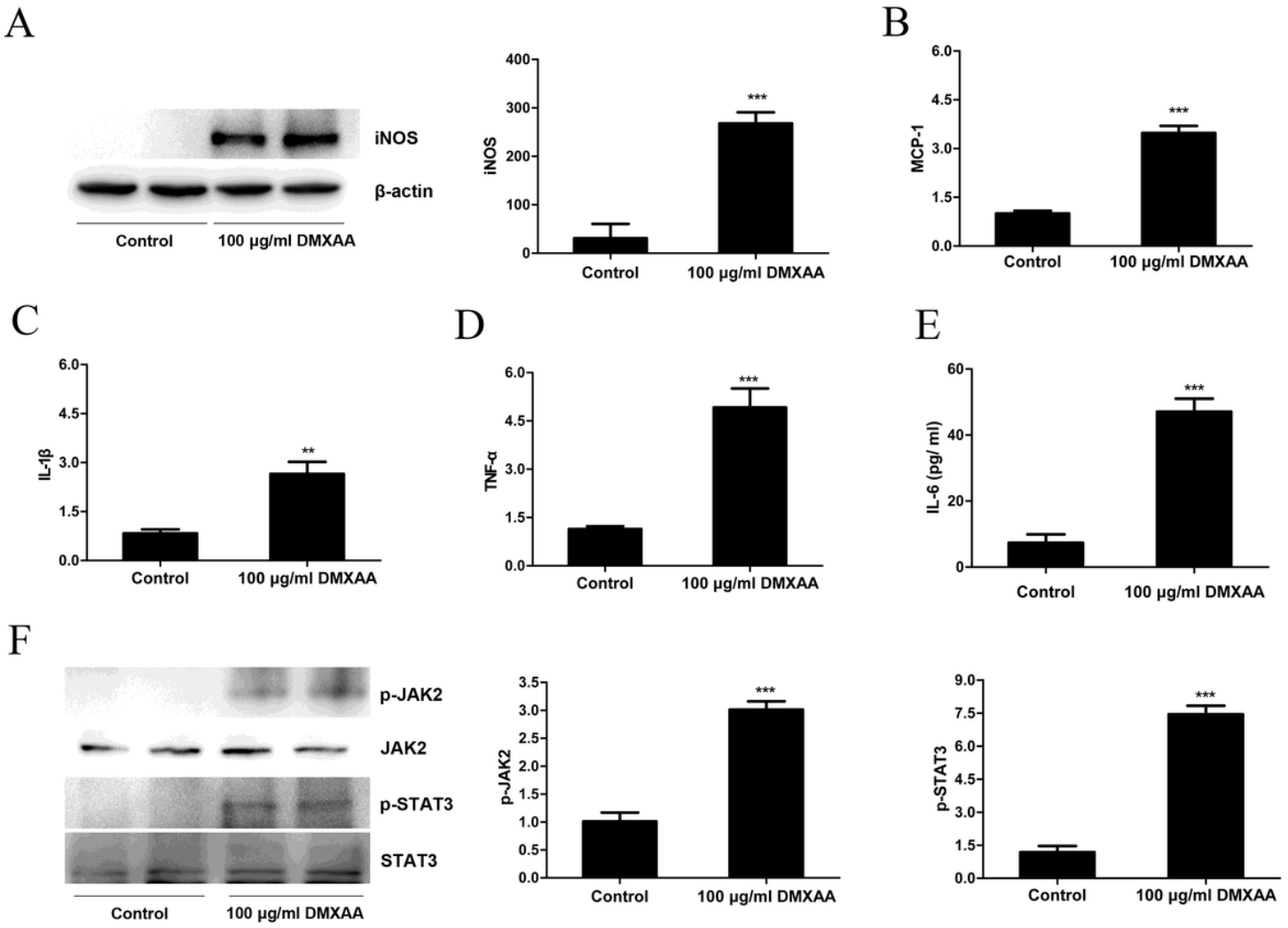

Figure 6

DMXAA significantly increased the expression of pro-inflammatory cytokines and phosphorylation of JAK2/STAT3. BV-2 cells were stimulated by DMXAA for 24 h. (A) The protein level of iNOS in BV-2 cells stimulated by DMXAA for 24 h. (B) Relative mRNA level of MCP-1 in BV-2 cells stimulated by DMXAA for 24 h. (C) Relative mRNA level of IL-1β in BV-2 cells stimulated by DMXAA for 24 h. (D) Relative mRNA level of TNF-α in BV-2 cells stimulated by DMXAA for 24 h. (E) BV-2 cells supernatants were collected at 24 h after DMXAA stimulation. IL-6 serum levels were quantified by ELISA. (F) BV-2 cells supernatants were collected at 24 h after DMXAA stimulation. IFN-β serum levels were quantified by ELISA. (G-I) The protein levels of p-JAK2 and p-STAT3 in BV-2 cells stimulated by DMXAA for 24 h. All data are presented as means ± SEM. (n=4 per group, ***P<0.001 compared with the Control group).

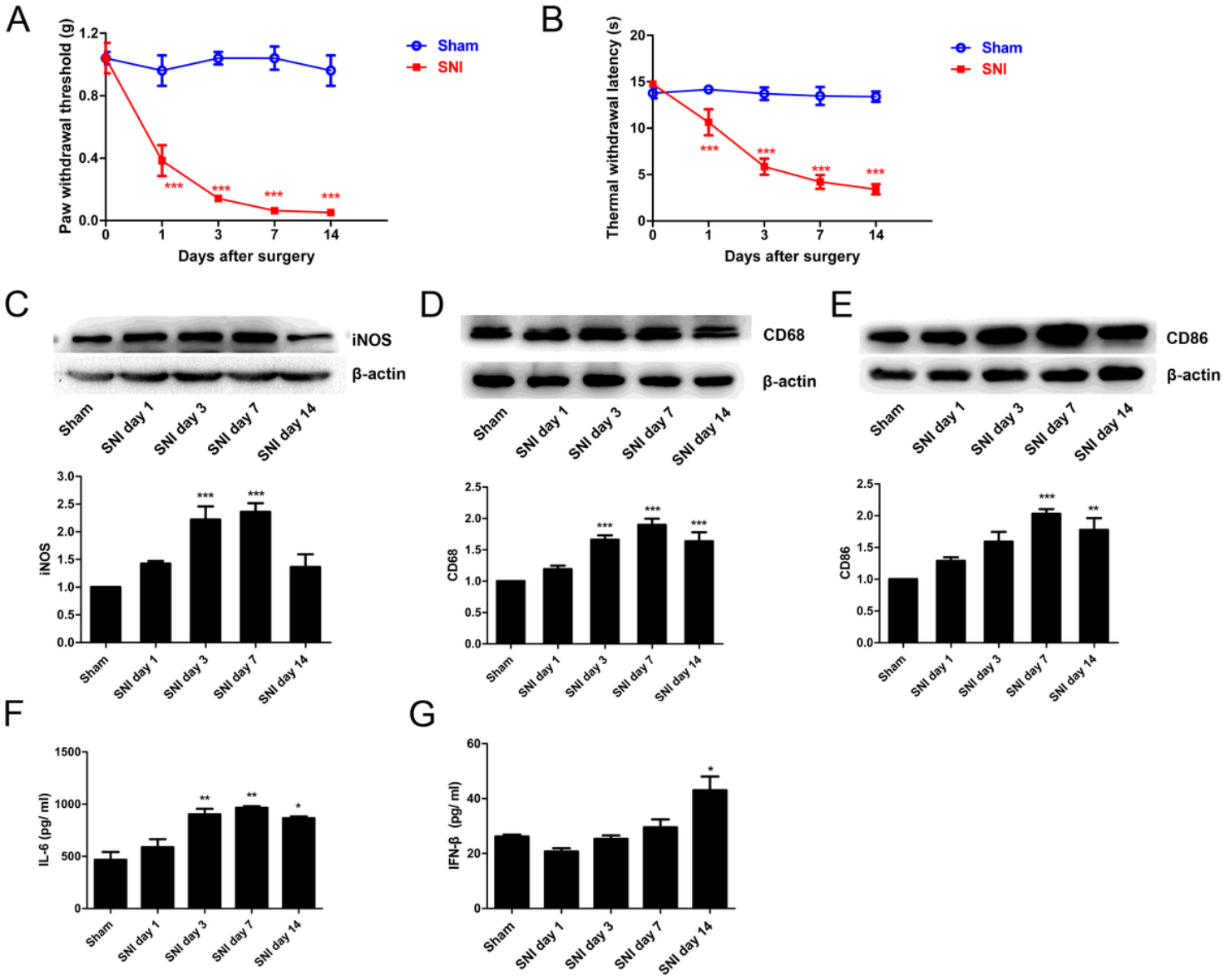

Figure 7

Time course of pain hypersensitivity and pro-inflammatory cytokines in the spinal cord following SNI. (A and B) Mechanical allodynia and thermal hyperalgesia were assessed in sham-operated and SNI-injured mice (n=5 per group). (C-E) Expression of M1 microglia markers (iNOS, CD68, CD86) in L4-5 spinal cord dorsal horn increased in a time-dependent manner after SNI. (n=5 per group). (F) The protein expression of IL-6 in the spinal cord dorsal horn was detected by Elisa analysis (n=3 per group). (G) The expression of IFN-β in the spinal cord dorsal horn was detected by Elisa analysis (n=3 per group) All data are presented as means ± SEM. (*P<0.05, **P<0.01, ***P<0.001 compared to sham-operated group).

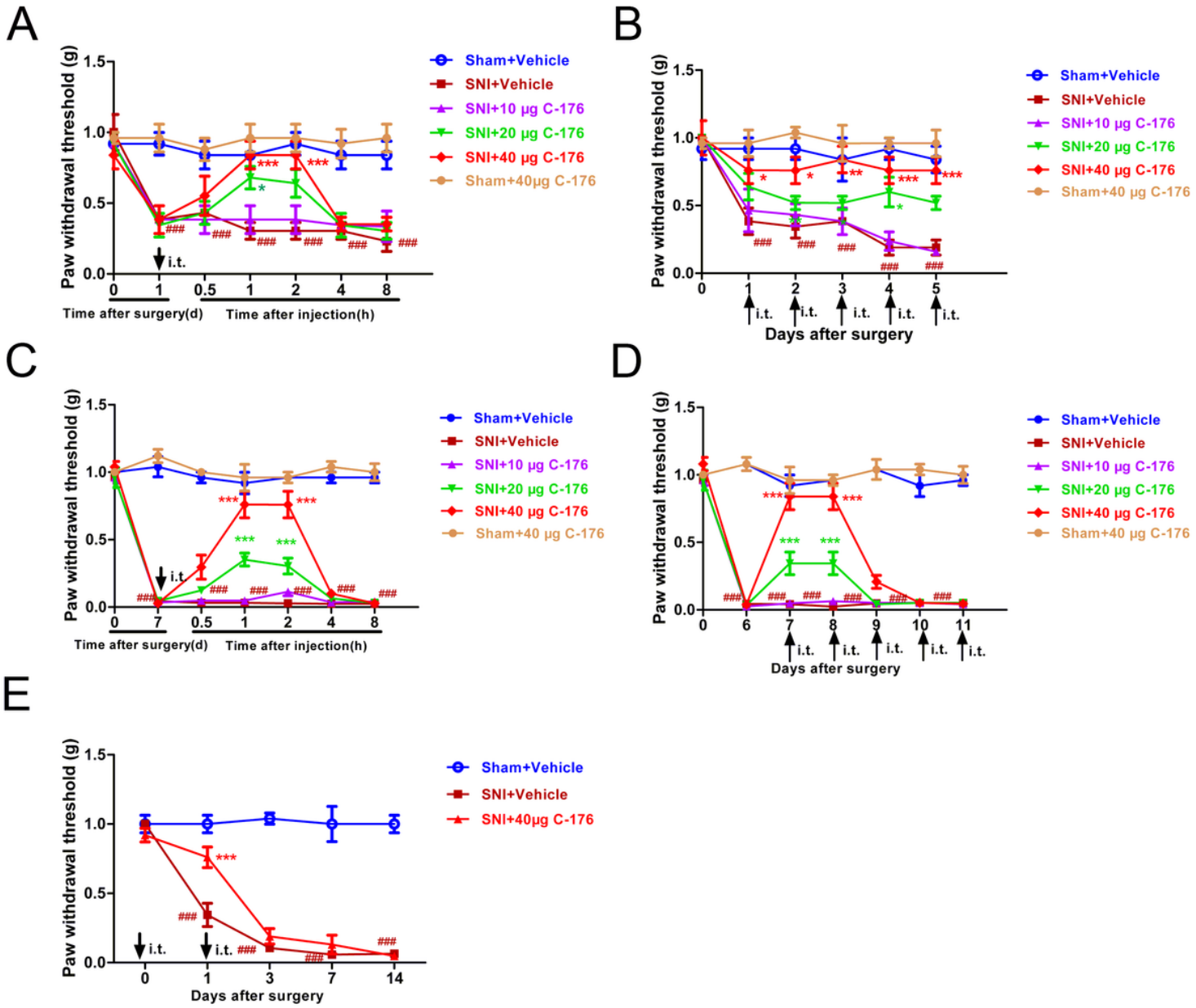

Figure 8

Early but not late C-176 injection attenuated SNI-induced mechanical allodynia. Mechanical allodynia was assessed in sham-operated mice with vehicle injection(Sham+Vehicle), SNI-injured mice with vehicle injection (SNI+Vehicle), SNI-injured mice with C-176 injection (SNI+C-176; 10, 20, 40 μg, i.t.) and sham-operated mice with C-176 injection (Sham+C-176; 40 μg, i.t.). (A) A single dose of C-176 (10, 20, 40 μg, i.t.) or Vehicle (5 μl, i.t.) was injected into sham mice and SNI-injured mice on day 1. Mechanical allodynia was measured at 0, 0.5, 1, 2, 4 and 8 h after single injection of C-176. (B) C-176 (40 μg, i.t.) was applied once daily for early phase from day 1 to day 5 following SNI. PWT was conducted at 1 h after C-176 injection from day 1 to day 5 following SNI. (C) A single dose of C-176 (10, 20, 40 μg, i.t.) or Vehicle (5 μl, i.t.) injected into sham mice and SNI- injured mice on day 7. Mechanical allodynia was measured at 0, 0.5, 1, 2, 4 and 8 h after single injection of C-176. (D) C-176 (40 μg, i.t.) was applied once daily for late

phase from day 7 to day 11 following SNI. PWT was conducted at 1 h after C-176 injection from day 7 to day 11 following SNI. (E) C-176 (40 μg, i.t.) was applied once daily at 0.5h before surgery and at day 1 after surgery. PWT was conducted at baseline and at day 1, 3, 7, 14 after SNI surgery. (n=5 per group, *P<0.05, **P<0.01, ***P<0.001 compared with the SNI+Vehicle group, ###P<0.001 compared with the Sham+Vehicle group).

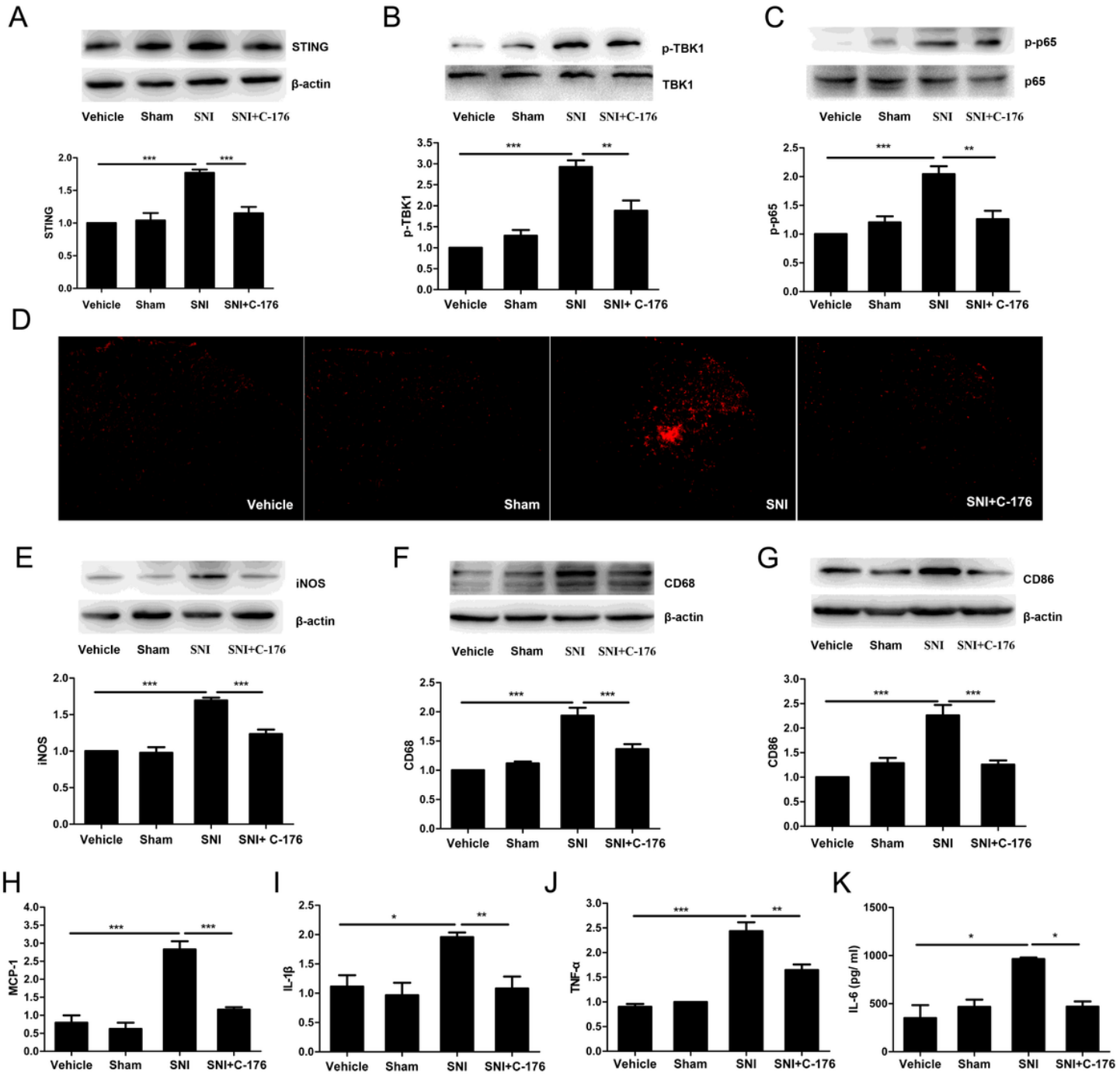

Figure 9

C-176 reduced microglia activation and proinflammatory cytokine expression in the spinal cord after SNI. (A-C) The protein level of STING, TBK1 phosphorylation, and NF-κB p65 phosphorylation in the L4-5 dorsal horn was detected using the sham-operated mice with vehicle administration (Sham), SNI-injured

mice with vehicle administration (SNI), SNI-injured mice with successive C-176 administration (SNI+C-176), and vehicle group as the negative control (Vehicle). (n=5 per group). (D) Representative images of immunofluorescence of Iba1 in the L4-5 dorsal horn of vehicle-operated control mice (Vehicle), SNI-injured mice (SNI) at 7 d after surgery, and SNI-injured mice with successive C-176 administration from day 1 to day 5 (SNI+C-176) (n=3 per group, bar=200 μm.) (E-G) The protein levels of M1 microglia markers (iNOS, CD68, CD86) in the L4-5 dorsal horn of vehicle-operated control mice (Vehicle), SNI-injured mice (SNI) at 7 d after surgery, and SNI-injured mice with C-176 administration (SNI+C-176). (n=5 per group). (H-J) The mRNA expression of MCP-1, IL-1β and TNF-α in the L4-5 dorsal horn of sham-operated mice (Sham), SNI-injured mice (SNI) at 7 d after surgery, and SNI-injured mice with successive C-176 administration (SNI+C-176). (n=5 per group). (K) The level of IL-6 was detected by Elisa analysis in the L4-5 dorsal horn of sham-operated mice (Sham), SNI-injured mice (SNI) at 7 d after surgery, and SNI-injured mice with successive C-176 administration (SNI+C-176). (n=5 per group). All data are presented as means ± SEM. Tissues were collected on day 7 after C-176 administration from day 1 to day 5. (*P<0.05, **P<0.01, ***P<0.001 compared with indicated group).

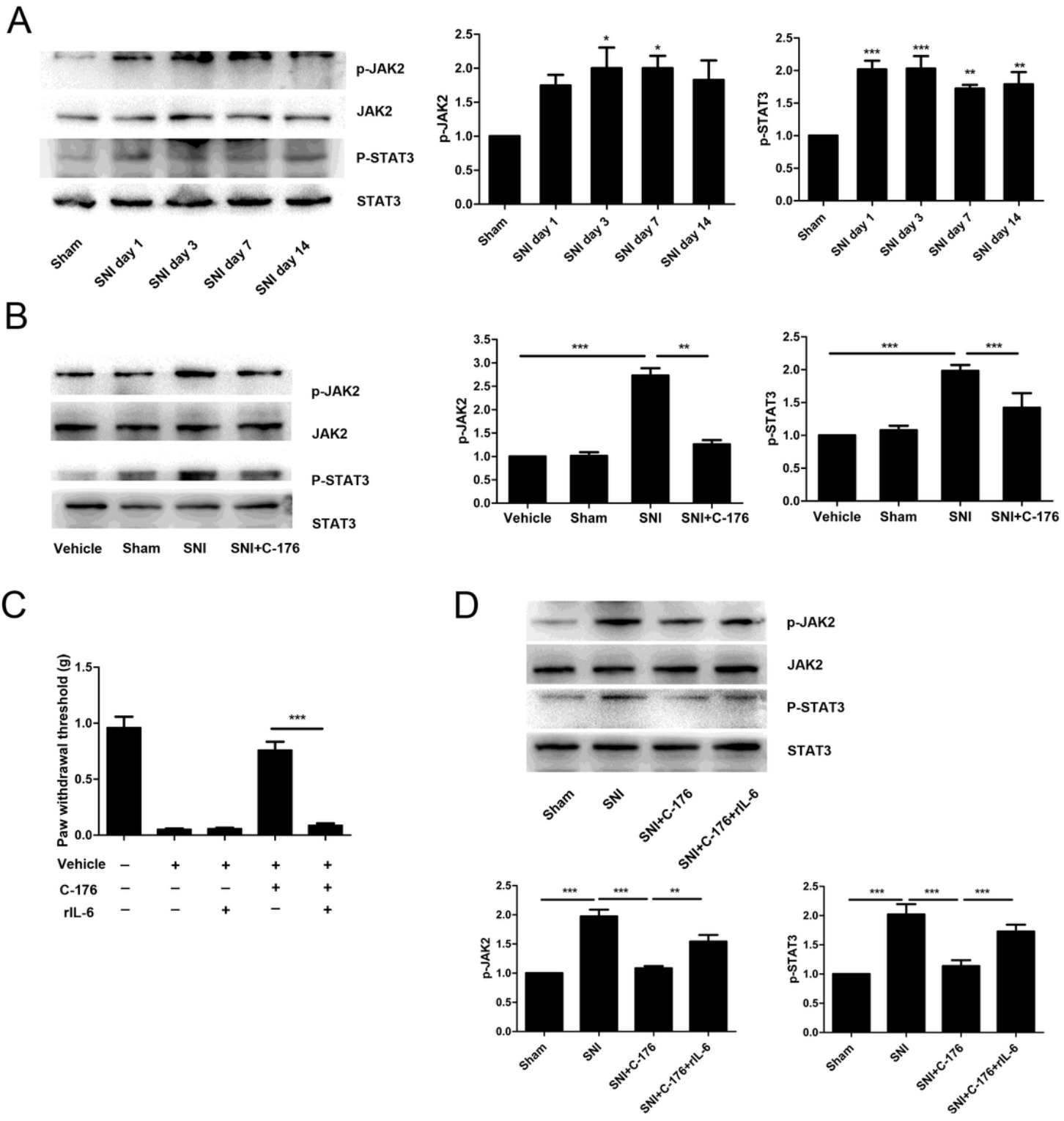

Figure 10

Intrathecal injection of C-176 attenuated SNI-induced mechanical allodynia via IL-6/JAK2/STAT3 expression. (A) Expression of p-JAK2/STAT3 in L4-5 spinal cord increased in a time-dependent manner compared with sham-operated mice. (B) The expression of p-JAK2/STAT3 in the L4-5 dorsal horn of sham-operated mice (Sham), SNI-injured mice (SNI) at 7 d after surgery, and SNI-injured mice with successive C-176 administration (SNI+C-176). (C) rIL-6 blocks the analgesic effects of C-176. C-176 (40

μg, i.t.) was given into SNI-injured mice with or without mice rIL-6 (100 ng, i.t.) from day 1 to day 5 ; and mechanical allodynia was examined at day 7 after surgery. (D) The expression of p-JAK2/STAT3 in the L4-5 dorsal horn from each group were measured after mice rIL-6 injection by western blotting. Data are expressed as mean ± SEM. (n=5 per group, *P<0.05; **P<0.01, ***P<0.001 compared with indicated group).

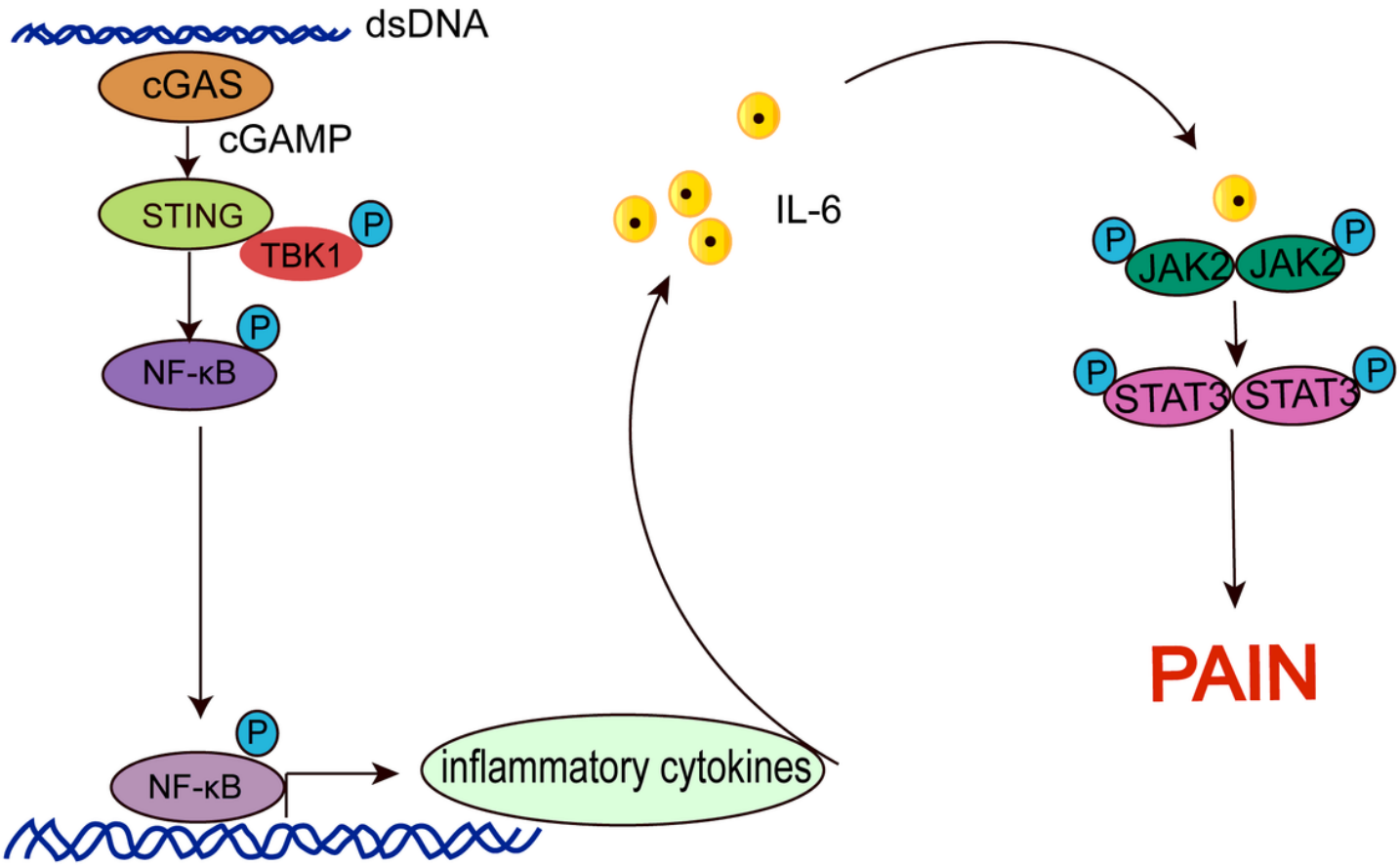

Figure 11

Schematic diagram of microglial STING/NF-κB/IL-6 regulated SNI-induced pain hypersensitivity. During the development of SNI, dsDNA was increased first and activate microglial STING. Upon activated, STING then recruits TBK1, and phosphorylated NF-κB, which subsequently promote the release of proinflammatory cytokines (such as IL-1β、IL-6 and TNF-α), resulting microglial activation and polarize into M1 phenotype exacerbating releasing of proinflammatory factors in the spinal cord dorsal horn. Moreover, the role of the main inflammatory factors IL-6 could promote pain hypersensitivity via JAK2/STAT3 axis in the spinal cord microglia.

Supplementary Files

This is a list of supplementary files associated with this preprint. Click to download.

- Supplementaryinformation.docx

- figureS1.tif